ELSEVIER

Polymer 42 (2001) 1143–1156

polymer

www.elsevier.nl/locate/polymer

Description of the tensile stress–strain behaviour of filler-reinforced rubber-like networks using a Langevin-theory-based approach. Part II

B. Meissner*, L. Matějka

Institute of Macromolecular Chemistry, Academy of Sciences of the Czech Republic, Heyrovsky Square 2, 162 06 Prague 6, Czech Republic

Received 17 January 2000; received in revised form 17 May 2000; accepted 13 June 2000

Abstract

The equation proposed and tested in previous papers (i.e. a combination of the Langevin-theory-based James–Guth equation with the phenomenological C_2 term of the Mooney–Rivlin equation, modified by introducing an additional empirical parameter) is shown to represent with a good success the experimental stress–strain dependences up to the break of filler-reinforced elastomeric networks when the concept of a strain-dependent finite extensibility parameter is used. The equation contains eight parameters (six of them are adjustable) and the accuracy of the data description is better than ca. 5%. Parameter values were determined for a number of styrene–butadiene networks reinforced with carbon black, precipitated silica, or silica generated in situ by the sol–gel method. Relations of the parameter values to the filler type and concentration are discussed.

Keywords: Tensile stress–strain dependence; Theory of rubbber elasticity; Filler reinforcement

1. Introduction

Our previous papers [1,2] have shown that the tensile stress–strain dependences (SSDs) of unfilled and filler-reinforced elastomeric networks, measured both at very low and at high strain rates, can be described in the low- and medium-strain range, by the JGmC2 equation. The JGmC2 equation is a combination of the two-parameter James–Guth equation [3–5] which is based on the Langevin elasticity theory, and of the modified [2] two-parameter C_2 term of the Mooney–Rivlin equation [6,7]. In the region of high strains, the stress–strain behaviour is more complex and can be described when introducing the concept of a strain-dependent finite extensibility parameter, λ_m [1,2]. This leads to the JGmC2L equation which is given in Appendix A together with an illustrating graph (Fig. 12). It is discussed in more detail in Part I of the present paper [2]. The JGmC2L equation is the JGmC2 equation in which the dependence of λ_m on the extension ratio λ (obtained by comparing the JGmC2 equation with experimental data) is described by a suitably chosen power function. The JGmC2L equation contains six adjustable parameters, three of them (n, C_1 and C_2) being determined from the low- and medium-strain behaviour, and the remaining three (λ_1, $\lambda_{m,1}$ and a) from the medium- and high-strain behaviour. The JGmC2L equation contains two additional quantities, $\lambda_{m,2}$ and λ_2, which are the coordinates of λ_m on λ dependence at the highest extension ratio applied, $\lambda = \lambda_2$. The JGmC2L equation has been shown in Part I [2] to give a good data representation, with maximum 4% deviation, of pre-strained networks, both on retraction and subsequent elongation. Under specific conditions of straining and network composition, the behaviour may simplify and the number of necessary parameters diminishes. For example, on retraction, the finite extensibility parameter appears to be virtually independent of strain and n often approaches 1.

In Part II of the present paper, the JGmC2L equation is compared with virgin stress–strain curves of filler-reinforced elastomeric networks, i.e. with data obtained on extension up to the break of hitherto undeformed specimens. In practice, such SSDs are the most commonly measured for use in quality control, material specification and in developmental studies.

2. Experimental

Most of the elastomeric networks described in Part I [2] were also used for the determination of the virgin SSDs up to the break in Part II. Their codes together with basic information on the type and concentration of filler are summarized in Table 1. Several other elastomeric materials

* Corresponding author. Tel.: +42-2-2040-3384; fax: +42-2-367981.
E-mail address: meissner@imc.cas.cz (B. Meissner).

0032-3861/01/$ - see front matter
PII: S0032-3861(00)00451-1

Table 1
Composition of elastomeric materials (VL, very low; L, low; M, medium; H, high. (Medium strain rate ~100%/min. All networks are based on an emulsion SBR, 23% of styrene.) (MT50 Fed network was crosslinked with dicumyl peroxide, all other networks were crosslinked by common sulfur/accelerator systems)

Code	Degree of crosslinking	Filler	Concentration of filler (phr)	Strain rate	Reference
SBR 0[a]	VL	–	–	H	[2]
SBR B[a]	L	–	–	H	[2]
SBR D[b]	M	–	–	M	[8]
F Kraus	M	Carbon black (HAF)[c]	(45)	H	[9]
GF Kraus	M	Graphitized[d]	(45)	H	[9]
MT50 Fed	M	MT	50	H	[10]
Hf20 Amb[a]	M	HAF	20	L	[11]
Hf30 Bue[a]	M	HAF	30	L	[12]
Hf40 Amb[a]	M	HAF	40	L	[11]
Hf60 Amb	M	HAF	60	L	[11]
V30 S05[a]	VL	Precipitated silica[e]	30	H	[13]
V35 S05 TEA[a]	L	Precipitated silica[f]	35	H	[2]
V40 S05[a]	L	Precipitated silica[f]	40	H	[2]
V40 S2[g]	M	Precipitated silica[f]	40	H	
VHS60 Pol	M	Precipitated silica[h]	60	H	[14]
SBR B SG[a]	L (SBR B)	Sol–gel silica	24	H	[2]

[a] More detailed information in Ref. [2].
[b] More detailed information in Ref. [1].
[c] Typical reinforcing carbon black, probably of the HAF type, in an estimated concentration of ca. 45 phr.
[d] Graphitized version of carbon black in an estimated concentration of ca. 45 phr.
[e] Precipitated silica of the Ultrasil VN3 type.
[f] Ultrasil VN3, specific surface area 200 m^2/g, Degussa, Germany.
[g] MOR (2-(morfolinosulfanyl)benzothiazole) 0.5, sulfur 2, TESPT silane (bis[3-(triethoxysilyl)propyl]tetrasulfide) 4 phr.
[h] Specially prepared precipitated silica with high structure, surface-hydrophobized with trimethylsilyloxy groups.

together with their codes and characteristics are also included.

3. Results and discussion

3.1. Carbon black-reinforced networks

Experimental SSDs of one unfilled and five carbon black-reinforced SBR networks (two of them were extended up to the break) are compared with the JGmC2L equation in Fig. 1; the curves are drawn using the parameter values given in Table 2. The fit of the curves to the experimental points may be regarded as very good, with deviations not exceeding 5%. A similar accuracy of data representation follows from the Mooney–Rivlin plot (Fig. 2) which optically accentuates the low-strain data. From the log(reduced stress) vs. λ plot in Fig. 3 it can be seen that the *relative* deviation of the experimental reduced stress from the fitted curve is approximately the same in the whole range of strain. On a very careful inspection, a small local irregularity in the form of a 'shoulder' can be found on some fitted curves slightly above the minimum of reduced stress, in the vicinity of λ_1: the first derivative has a small maximum closely followed by a small minimum (see e.g. curve 2 in Fig. 3 and curve 6 in Figs. 2 and 3). This effect is obviously due to the limited ability of the power function to give a sufficiently accurate description of the experimentally determined dependences of λ_m on λ. By slightly varying the values of λ_1, $\lambda_{m,1}$, and a, the magnitude of the 'shoulder' can be reduced at the expense, however, of the quality of the overall fit to data at higher strains.

The network SBR D and the respective unfilled networks of Hf20 Amb, Hf40 Amb, Hf60 Amb can be expected to have a similar (medium) degree of chemical crosslinking. In the series of networks SBRD, Hf20 Amb, Hf40 Amb, and Hf60 Amb which were all tested using a low or very low strain rate, the concentration of the HAF carbon black increases (0, 20, 40, 60 phr) and the parameter values show the following tendencies.

n monotonically increases from unity to a large value of 9.2, thus reflecting an increasing degree of filler particle–particle interconnectivity; with even small pre-strains, such interconnections are destroyed and n is diminished significantly (cf. Part I [2]).

C_1 increases monotonically (roughly, 0.14, 0.2, 0.3, 0.5 MPa) and rather steeply; in theory, it should be proportional to the concentration of network junctions bearing a load which increases with strain; therefore, they may be denoted as stable junctions. Some of these junctions, however, do not survive the first extension and do not appear to be active any longer on repeated extensions (cf. Part I [2]).

C_2 increases monotonically (0.19, 0.21, 0.25, 0.32 MPa)

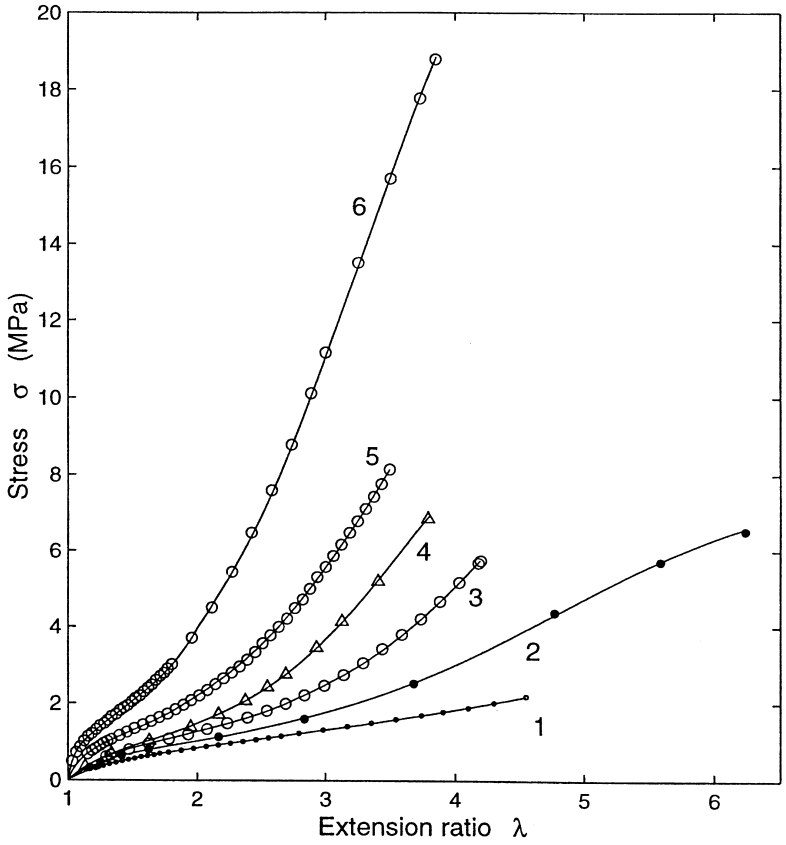

Fig. 1. Comparison of experimental SSDs of one unfilled and five carbon black-reinforced networks (points) with the JGmC2L equation (curves). For parameter values, see Table 2. (1) SBR D; (2) MT50 Fed; (3) Hf20 Amb; (4) Hf30 Bue; (5) Hf40 Amb; (6) Hf60 Amb. SSDs 1, 2, 6 up to break.

but less steeply than C_1, i.e. C_2/C_1 decreases with the HAF carbon black concentration (1.4, 1.1, 0.9, 0.65); C_2 seems to be less affected by pre-strain than C_1; on retraction and second extension, C_2/C_1 appears to be higher than on the first extension (cf. Part I, Table 6). If C_2 is due to some kind of non-stable junctions (sliding entanglements, slip-links [15,16], those which on the first extension bear a non-increasing load at extension ratios higher than, say 3, then the latter finding would lead to the conclusion that they are able to survive pre-strain with less damage than the more stable junctions contributing to C_1.

$\lambda_{m,1}$ monotonically decreases (5.6, 3.9, 2.8, 2.6) thus indicating a monotonic decrease in network mesh size and reflecting a decrease in the extensible rubbery matrix

Table 2
Parameters of the JGmC2L equation and other properties of carbon black-reinforced networks

Parameter	SBR D	MT50 Fed	HF20 Amb	HF30 Bue	HF40 Amb	HF60 Amb
n	1.0	1.0	1.60	1.26	4.20	9.20
C_1 (MPa)	0.135_6	0.093	0.198	0.173	0.290	0.490
C_2 (MPa)	0.187	0.34	0.215	0.272	0.250	0.320
λ_1	2.50	2.46	2.75	1.99	1.90	2.00
λ_2	4.51[a]	6.23[a]	4.20	3.79	3.50	3.85[a]
$\lambda_{m,1}$	5.60	3.5	3.93	2.90	2.80	2.63
$\lambda_{m,2}$	6.79	6.7	4.755	4.093	3.875	4.16
a	1.10	1.25	1.40	1.42	1.35	1.23
σ_b[b] (MPa)	2.2	6.58				18.8
C_2/C_1	1.38	3.66	1.09	1.57	0.86	0.65
D	0.21	0.56	(0.22)	(0.39)	(0.37)	0.48
k	0.59	0.85	(0.57)	(0.66)	(0.67)	0.83

[a] Break.
[b] σ_b = stress at break.

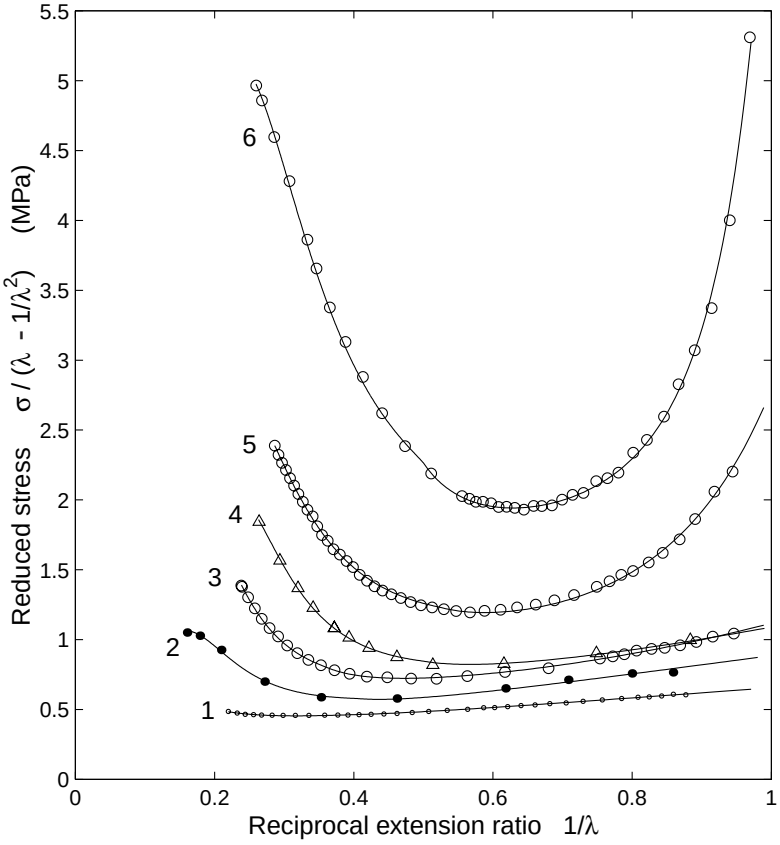

Fig. 2. Data and curves of Fig. 1 in the Mooney–Rivlin coordinates.

fraction in the material; a similar behaviour can be expected for $\lambda_{m,2}$, λ_2.

The total change of the finite extensibility parameter ε_m ($= \lambda_m - 1$) with extension relative to its maximum value $\varepsilon_{m,2}$ ($= \lambda_{m,2} - 1$), is given by

$$D = (\lambda_{m,2} - \lambda_{m,1})/(\lambda_{m,2} - 1)$$

The average slope of the dependence of λ_m on λ was defined in Part I by

$$k = (\lambda_{m,2} - \lambda_{m,1})/(\lambda_2 - \lambda_1)$$

With increasing concentration of the HAF carbon black, both D and k increase, i.e. the extent of the strain-induced growth of the finite extensibility parameter (of the network mesh size) becomes more and more pronounced. D may receive contributions both from the matrix (sliding entanglements) and from the filler–matrix interphase (disruption or sliding of filler–matrix contacts). Kraus mentions one more relaxational mechanism operating at high strains, the dewetting of rubber from the filler surface. This causes the slope of the stress–strain curve to diminish [9]. This effect is visible in Fig. 1 where the two SSDs tested up to the break (60 phr HAF black, curve 6, and 50 phr MT black, curve 2) both have two inflection points. The first one (upturn) is the finite extensibility effect while the other, a decrease in slope beginning at an elongation some 150% lower than the elongation-at-break, can perhaps be ascribed to the dewetting effect while micro-voiding can also be a contributing factor.

The reinforcement of SBR by the low-surface-area MT black (curve 2 in Figs. 1–3) cannot be unambiguously compared with the reinforcement by the HAF carbon black since there are differences in the crosslinking systems used (peroxide vs. sulfur). Some effects, however, seem obvious: at a comparable filler concentration level, n of the MT black-containing network is significantly smaller ($\sim$1), C_1 is small (it may not be much larger than C_1 of the corresponding unfilled peroxide network), C_2 is comparable with, and C_2/C_1 is much larger than that of the HAF black-containing network. In this last respect, the MT50 Fed network resembles the unfilled SBR networks. Lower C_1 should be accompanied by a larger network mesh size and, not unexpectedly, larger values of λ_1, λ_2, $\lambda_{m,1}$ and $\lambda_{m,2}$, are obtained in the presence of MT black. On the other hand, the *relative* change in the network mesh size (of the finite extensibility parameter) with strain, when expressed by D, is comparable with that of the HF60 Amb network.

3.2. The effect of graphitization of carbon black

In a review article, Kraus compared a typical stress–strain

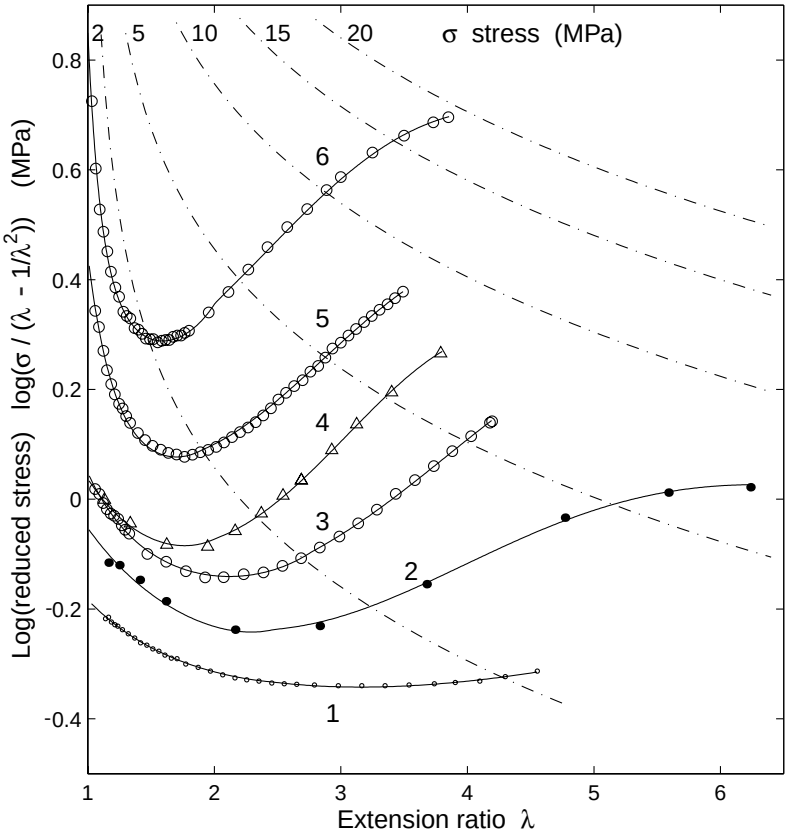

Fig. 3. Data and curves of Fig. 1 in the coordinates log(reduced stress) vs. extension ratio.

curve of a carbon black-reinforced vulcanizate (F Kraus) with the SSD of a network filled with a graphitized version of that carbon black (GF Kraus, Fig. 12 in Ref. [9]). The Kraus curves are reproduced in Fig. 4 as a series of experimental points. It should be noted that below some 100% elongation, the relative error in stress read from the Kraus curves increases. This uncertainty may influence the calculated values of n and C_2, (and to some extent, of C_1) but the conclusions based on the high-strain data will remain virtually unaffected.

The Kraus experimental data in Fig. 4 are described by the JGmC2L equation (full curves) very well using parameter values given in Table 3. The SSDs of Fig. 4 are replotted in coordinates log(reduced stress) vs. λ in Fig. 5 where the data on an unfilled network SBR B — the strain-at-break of which is comparable with that of the network GF Kraus — are included. The dashed curves indicate the range in which the high-strain behaviour changes as a result of the strain-induced increase in the finite extensibility parameter from its low initial value ($\lambda_{m,1}$) to its highest final value ($\lambda_{m,2}$).

The most interesting result following from Figs. 4 and 5 is the rather simple high-strain behaviour of the network GF Kraus that contains graphitized carbon black. Its SSD is rather close to the prediction of the James-Guth equation at high strains, where the *relative* contribution of the C_2 term to stress (Fig. 4, curve 2c) becomes very small. The strain-induced relative change in λ_m is surprisingly small and $D = 0.086$ is the lowest value so far obtained for networks extended up to the break, both unfilled and filler reinforced (cf. Tables 3 and 4). The values of D of unfilled networks range from ca. 0.15 to 0.22 while D of the F Kraus network containing the non-graphitized carbon black is about three times higher (0.63). Graphitization eliminates strong carbon black/polymer links and greatly decreases the stress at which dewetting is observed [9]. In the absence of strong localized surface bonds, molecular slippage is also enhanced and, according to Kraus, these effects keep the stress from rising rapidly until very high elongations are attained [9]. In accord with these arguments, graphitization should be expected to lead to a decrease in C_1 and C_2, and to an increase in λ_1 and $\lambda_{m,1}$. Inspection of the parameter values of F Kraus and GF Kraus networks confirms this. The fact that graphitization also results in a very low D could mean that dewetting is substantially complete at λ_1 and, therefore, ceases to contribute in an increasing manner to the decrease in the slope of the stress–strain curve at extension ratios higher than λ_1; indeed, no second inflection point is observed. Why the D value of the network containing graphitized carbon black is even lower than that of the unfilled networks does not seem clear at present. The value of k of the GF Kraus network (0.53) lies in the same region as those of the unfilled networks (0.47–0.59) while being substantially lower

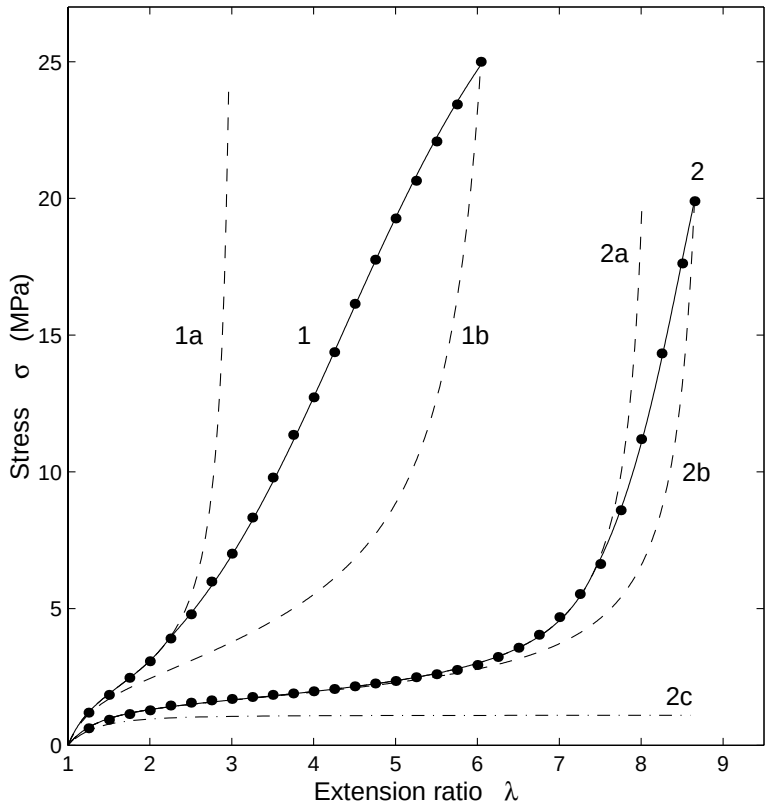

Fig. 4. Comparison of experimental SSDs up to break (points) with the JGmC2L equation (curves), the effect of graphitization. For parameter values, see Table 3. (1) F Kraus; (2) GF Kraus. 1, 2: λ_m changing from $\lambda_{m,1}$ to $\lambda_{m,2}$. 1a, 2a: Constant $\lambda_m = \lambda_{m,1}$. 1b, 2b: constant $\lambda_m = \lambda_{m,2}$. 2c: stress contribution to curve 2 given by the modified C_2 term.

than k in the presence of a non-graphitized carbon black (0.91).

3.3. Reinforcement by precipitated and in situ generated silica

Fig. 6 shows the SSD up to the break of one unfilled, very lightly crosslinked network, SBR 0, and of six networks containing silica. Four of them are reinforced by precipitated silica of the Ultrasil VN3 type; V35 S05 TEA network contains a triethanolamine activator, V40 S05 and V40 S2 networks contain a TESPT silane coupling agent. The VHS60 Pol network is reinforced by a specially prepared precipitated silica with a high structure and its surface is hydrophobized. The SBR B SG network is based on the silane-containing unfilled SBR B network. The silica particles were generated in situ using the sol–gel process. Curves in Fig. 6 are fitted to the experimental points using the JGmC2L equation and parameters given in Table 4. Again, a successful data representation is obtained and this is apparent both in linear coordinates (Fig. 6) which put emphasis on high-strain data and in the Mooney–Rivlin plot (Fig. 7) where the low-strain data are accentuated. In Fig. 8, the log(reduced stress) is plotted vs. strain normalized with respect to strain-at-break. Inspection of the parameter values in Table 4 reveals the following facts.

Table 3
Parameters of the JGmC2L equation and other properties of carbon black-reinforced networks. Effect of graphitization

Parameter	F Kraus	GF Kraus	SBR B
n	1.80	1.0	1.0
C_1 (MPa)	0.44	0.095	0.043_8
C_2 (MPa)	0.41	0.55	0.23_8
λ_1	2.22	7.38	5.10
λ_2	6.04	8.65	8.95
$\lambda_{m,1}$	3.08	8.24	8.0
$\lambda_{m,2}$	6.56_5	8.91_8	10.0
a	1.18	1.60	1.20
σ_b (MPa)	25	20	3.23
C_2/C_1	0.93	5.8	5.43
D	0.63	0.086	0.22_2
k	0.91	0.53	0.52

n increases with precipitated silica concentration and — as supported by more data not shown here — diminishes when the silane coupling agent is added into the rubber compound. Not unexpectedly, surface hydrophobization (VHS60 Pol) leads to a drastic reduction of n. On the other hand, the very high value of n of the SBR B SG network (together with its high C_2) suggests that our in situ generated silica particles are highly interconnected. Such "filler-networking" may be a step in a bicontinuous network formation [16]. It is interesting to see that a value of

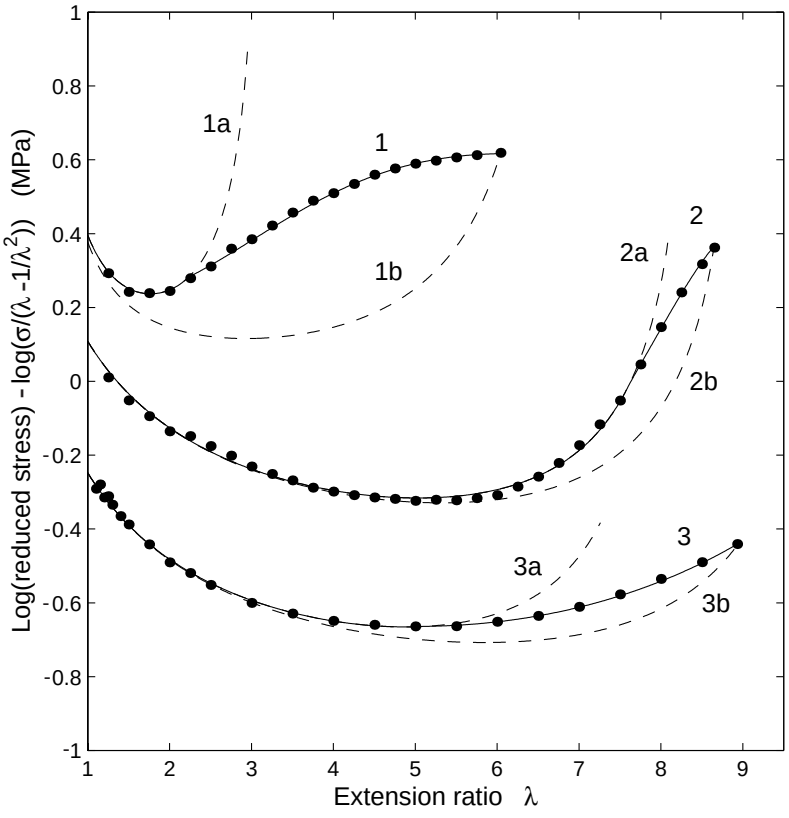

Fig. 5. Data and curves of Fig. 4 in coordinates log(reduced stress) and extension ratio (curve 2c omitted). Data and curve 3: SBR B. For parameter values, see Table 3.

n higher than unity may appear even in unfilled networks. It was obtained in the very lightly crosslinked network, SBR 0.

C_1 shows a tendency to increase with silica concentration (SBR B: 0.0438 MPa; V40 S05: 0.165 MPa; vulcanizing system and the silane additive are the same) but this effect may be obscured by the interference of silica acidity with the vulcanizing system (SBR 0: 0.0171 MPa; V30 S05: 0.013 MPa; vulcanizing system the same, no additive). Addition of triethanolamine to V30 S05 (with only a minor increase in silica loading) leads to a significant increase in C_1 (V35 S05 TEA: 0.042 MPa). Surface-hydrophobized silica, in spite of its high loading, gave a much lower C_1 (VHS60 Pol: 0.093 MPa) than untreated silica in a silane-containing system (V40 S05: 0.165 MPa; V40 S2: 0.235 MPa). In situ silica gives only a slightly higher C_1 (SBR B SG: 0.19 MPa) than precipitated silica with a comparable matrix (V40 S05: 0.165 MPa) but, contrary to precipitated silica, it is able to preserve or even increase the level of C_1 on retraction and subsequent elongation [2].

C_2 of the five networks containing precipitated silica is

Table 4
Parameters of the JGmC2L equation and other properties of silica-reinforced networks

Parameter	SBR 0	V30 S05	V35 S05 TEA	VHS60 Pol	V40 S05	V40 S2	SBR B SG
n	1.70	2.8	6.0	2.1	4.0	6.0	10.0
C_1 (MPa)	0.017_1	0.013	0.042	0.093	0.165	0.235	0.19
C_2 (MPa)	0.176	0.320	0.330	0.41	0.448	0.370	2.42
λ_1	9.8	8.60	5.00	4.65	3.05	2.72	1.85
λ_2	15.18	17.6	12.75	8.70	8.25	6.45	5.42
$\lambda_{m,1}$	14.15	11.2	7.45	6.56	4.45	3.54	2.60
$\lambda_{m,2}$	16.7	18.105	13.15	8.878	8.80	6.77	5.68
a	1.10	1.17	1.10	1.48	1.19	1.165	1.13
σ_b (MPa)	2.43	6.3	12.7	28.4	16.4	23.4	20.8
C_2/C_1	10.3	24.6	7.9	4.4	2.7	1.57	12.7
D	0.16	0.40	0.47	0.29	0.56	0.56	0.66
k	0.47	0.77	0.74	0.57	0.84	0.87	0.86

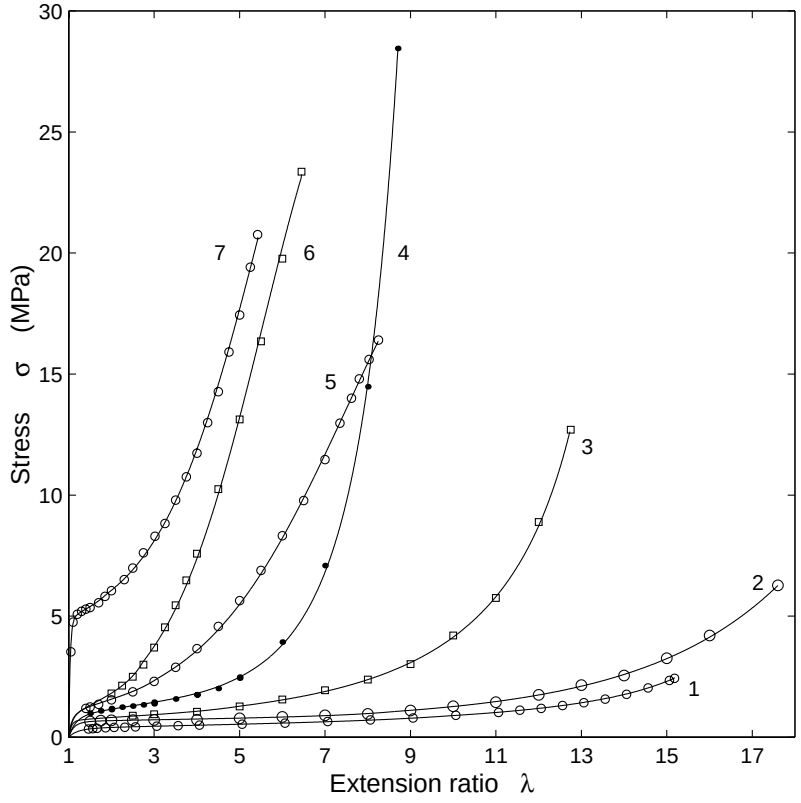

Fig. 6. Comparison of experimental SSDs up to break (points) with the JGmC2L equation (curves) for one unfilled and six silica-reinforced networks. For parameter values, see Table 4. (1) SBR 0; (2) V30 S05; (3) V35 S05 TEA; (4) VHS60 Pol; (5) V40 S05; (6) V40 S2; (7) SBR B SG.

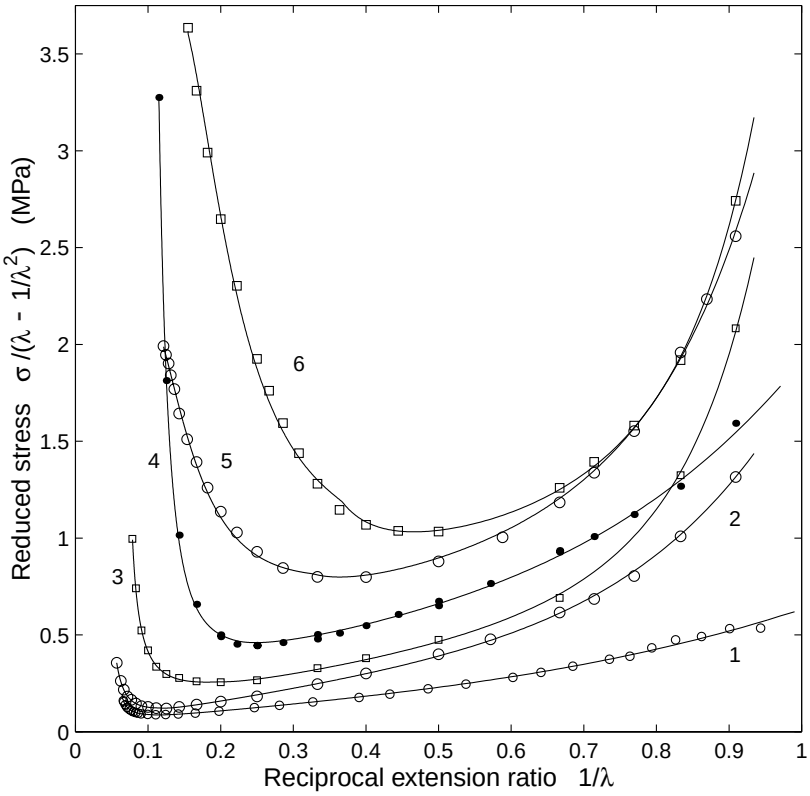

Fig. 7. Data and curves of Fig. 6 in the Mooney–Rivlin coordinates. Data and curve 7 omitted.

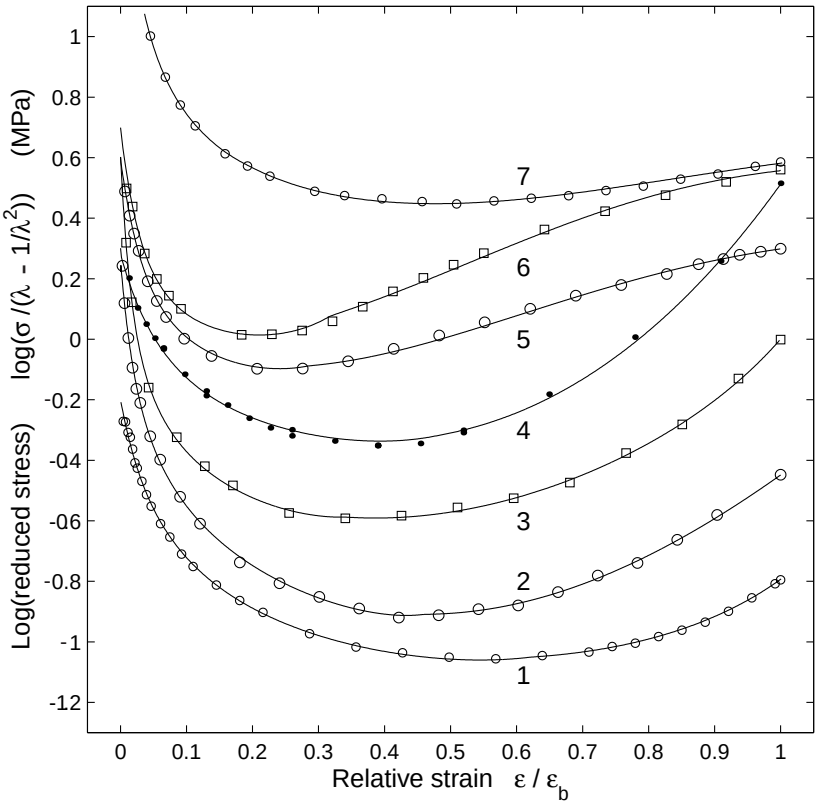

Fig. 8. Data and curves of Fig. 6 in coordinates log(reduced stress) and relative strain (i.e. strain normalized with respect to strain-at-break).

rather insensitive to silica concentration, surface hydrophobization, presence of additives, degree of crosslinking; it lies in a rather narrow range from 0.32 to 0.45 MPa. On the other hand, the in situ generated silica imparts an enormous increase in C_2, up to 2.42 MPa. This effect, however, is strain sensitive; on retraction, C_2 dropped to one-tenth of its initial value (0.25 MPa) while on subsequent elongation, an increase to 0.62 MPa was observed [2]. The high initial reduced stress of the in situ reinforced vulcanizate with its rigid network of silica particles could possibly be modelled by following the proposals of Boyce et al. [17] and Wu and van der Giessen [18] in their treatments of yield and strain hardening of glassy polymers. The model introduces an additional force acting in parallel with those due to rubber elasticity, which may be ascribed to friction or structural changes.

C_2/C_1 behaves in a way similar to that in the presence of carbon black: it tends to decrease with increasing degree of crosslinking and increasing concentration of precipitated silica. Therefore, the V30 S05 network with its low silica concentration and very low degree of crosslinking shows an extremely high $C_2/C_1 = 24.6$, a value not observed so far. The network reinforced with silica in situ also has a very high C_2/C_1 ratio (12.7).

$\lambda_{m,1}$ and $\lambda_{m,2}$ (λ_1 and λ_2 as well) decrease with increasing silica loading and crosslinking degree, similarly to the behaviour observed in carbon black-containing networks. These parameters reflect the network mesh size and the reciprocal density of network junctions of all kinds that have survived up to large strains. On the other hand, the C_1 parameter reflects the density of network junctions that are effective at low and medium strains. Nevertheless, some degree of correlation between the network mesh size at high strains and the density of network junctions at low and medium strains should exist, and this can be seen in Fig. 9. A reasonably satisfactory correlation (large points) with a theoretical slope of -0.5 (see below) is obtained with data on ten networks, both filled and unfilled:

$$\log \lambda_{m,2} = 0.382 - 0.5 \log C_1 \quad (1)$$

$$\lambda_{m,2}^2 = 5.81/C_1 \quad (2)$$

This result is probably due to mutually compensating effects that fillers exert on C_1 (increase) and $\lambda_{m,2}$ (decrease). The four small points in the region of high C_1, which deviate from the correlation to the right, belong to highly reinforced networks (40 phr silica + silane, 60 and 45 phr HAF carbon black).

The empirical observation (2) can be compared with the relations following from the Langevin elasticity theory for the finite extensibility parameter and modulus of perfect unfilled networks ($C_2 = 0$) :

$$\lambda_m^2 = M_c/M_s \quad (3)$$

$$2C_1 \times 10^6 = \rho RT/2M_{cf,p} \qquad \text{phantom network} \quad (4)$$

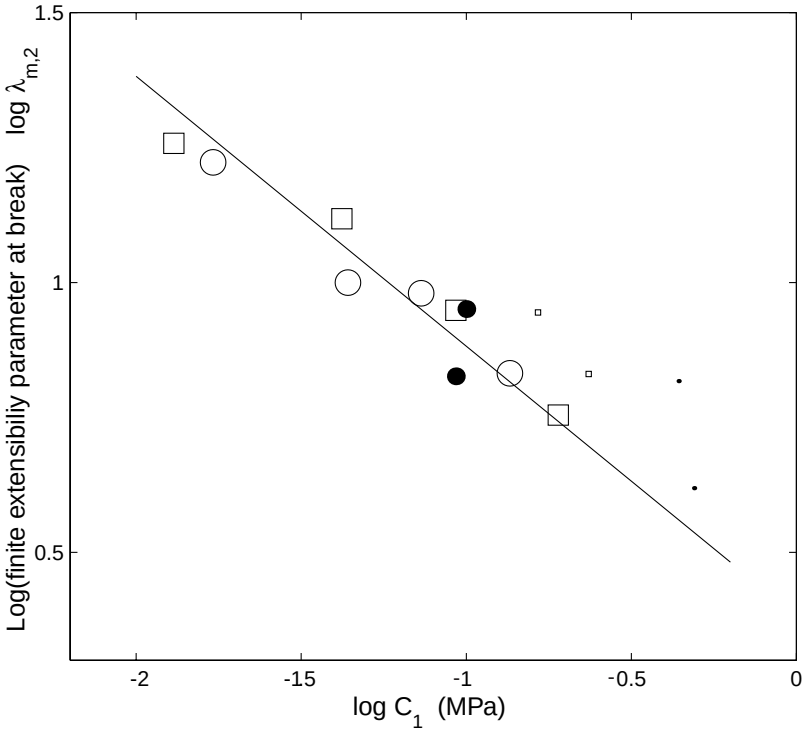

Fig. 9. Correlation of finite extensibility parameter at break with C_1 parameter (points) in a double logarithmic plot. Straight line is drawn according to Eq. (1). Circles: unfilled networks SBR 0, B, C [1], D. Squares: V30 S05, V35 S05 TEA, VHS60 Pol, SBR B SG. Full circles: MT50 Fed, GF Kraus. Small squares: V40 S05, V40 S2. Small full circles: Hf60 Amb, F Kraus.

M_c is the molar mass of network chains between network junctions and M_s is the molar mass of a statistical segment. In Eq. (4), C_1 is given in MPa units and $M_{cf,p}$ can be identified with the molar mass of network chains between network junctions operating at low and medium strains; for perfect unfilled networks it should be equal to M_c. Real networks contain strain-dependent imperfections of various type and, generally, $M_{cf,p}$ may be expected to differ from M_c. Let us assume that $M_{cf,p}$ and M_c differ by an empirical factor, b

$$M_{cf,p} = M_c/b \tag{5}$$

and that the value of $\lambda_{m,2}$ is determined by M_c/M_s

$$M_c/M_s = \lambda_{m,2}^2 \tag{6}$$

Combining Eqs. (5) and (6) with the empirical correlation (2) we obtain

$$M_s = \rho RTb/(4 \times 5.81 \times 10^6)$$

Taking a probable medium value for the density of unfilled and filled networks, $\rho = 10^3$ kg/m^3, and assuming $b = 1$, we get an estimate of $M_s = 0.105$ kg/mol. For an affine network $2C_1 \times 10^6 = \rho RT/M_{cf,a}$ and with analogous reasoning we arrive at $M_s = 0.21$ kg/mol. This is close to the value 0.19 kg/mol quoted and used by Klüppel and Heinrich [8].

The relative change, D, of the finite extensibility parameter with strain of the high-strength networks V40 S05, V40 S2, SBR B SG, is similar (0.55–0.65) to that of the high-strength carbon black-containing networks. Surface hydrophobization of silica by reacting the silanol groups to trimethylsilyloxy groups parallels the effect of graphitization of carbon black. It leads to a reduction of strong polymer/filler links and, therefore, the observed low value of $D = 0.29$ of the VHS60 Pol network (though not as low as that of the GF Kraus network) is in accord with what one should expect.

The course of the SSD at high strains of the VHS60 Pol network (Fig. 6) is at first sight distinctly different from those of the high-strength networks V40 S05, V40 S2, SBR B SG. The slope $d\sigma/d\lambda$ is higher and does not show any signs of a dewetting-induced decrease with strain. An interesting comparison of the SSDs of silica-reinforced networks is shown in Fig. 8. At high strains approaching break, the log(reduced stress) of the silane-containing networks (curves 5–7) levels off while those of the networks containing triethanolamine or no additive tend to increase.

While graphitization results, as a rule, in a decrease in tensile strength, the VHS60 Pol network attains an unusually high tensile strength. This may be ascribed to the very high structure of the silica rather than to the effects of surface treatment.

A comparison of experimental data with the JGmC2L equation presented in Sections 3.1–3.3 shows that the parameter values obtained offer a full and consistent information

on the tensile stress–strain behaviour up to the break. With an automated parameter acquisition, their utilization for practical purposes (e.g. monitoring the time uniformity of a technological process) seems feasible. They can be expected to signal the batch-to-batch variations similarly to the conventional parameters (moduli, stress and strain at break) but, on top of that, they have the advantage of giving a logically interpreted information on the whole SSD including, e.g. the behaviour at low strains (values of n, C_2) which is seldom checked in practice though being a potential source of valuable information.

3.4. Dependence of the finite extensibility parameter on strain

The dependence of the finite extensibility parameter ε_m ($= \lambda_m - 1$) on the strain ε ($= \lambda - 1$) is obtained from a comparison of the experimental SSD with the JGmC2 equation [1,2]. It can be satisfactorily described by the power function given previously (Eq. (5) in Part I of Ref. [2], Eq. (A2) in Appendix A). For a comparison of various networks, it is advantageous to define a ratio, P, of strain to finite extensibility parameter:

$$P = \varepsilon/\varepsilon_m = (\lambda - 1)/(\lambda_m - 1)$$

At low and medium strains, where the finite extensibility parameter is strain-independent, P increases linearly with increasing strain, the slope being given by the reciprocal of the initial finite extensibility parameter, $1/\varepsilon_{m,1}$. With no strain-induced increase in ε_m, the highest hypothetically attainable strain-at-break would be $\varepsilon_{m,1}$. If ε_m is able to increase with increasing strain to above $\varepsilon_{m,1}$, the slope of the dependence of P on ε begins to decrease and the P vs. ε dependence tends to level off. This is shown in Fig. 10 where two unfilled and seven filler-reinforced networks are compared. A high strain-at-break is reached if

(a) $\varepsilon_{m,1}$ is high; the additional increase to $\varepsilon_{m,2}$ (i.e. the value of D) need not be too large. Networks containing graphitized carbon black (curve 1) and surface-hydrophobized silica (curve 4) behave in this way. High $\varepsilon_{m,1}$ is usually associated with a low C_1 and a low stiffness at low strains.
(b) in the case of a low $\varepsilon_{m,1}$, relaxational mechanisms are operating in the network that allow the network mesh size and the finite extensibility parameter to increase with increasing strain; D should now be large. High values of D together with rather large strains-at-break were obtained for MT50 Fed and SBR B SG.

In both cases, the attainment of a high value of P at break ($P_b = \varepsilon_2/\varepsilon_{m,2}$) not only indicates a higher strain-at-break but, more significantly, it is a prerequisite for the attainment of a high stress-at-break. High P_b indicates that the stress has climbed sufficiently high on the steeply increasing portion of the SSD where a small increase in strain leads to a high increase in stress. High values of P_b were obtained for VHS60 Pol (0.977), GF Kraus (0.966), V40 S2 (0.945), SBR B SG (0.944), all having stress-at-break in the region

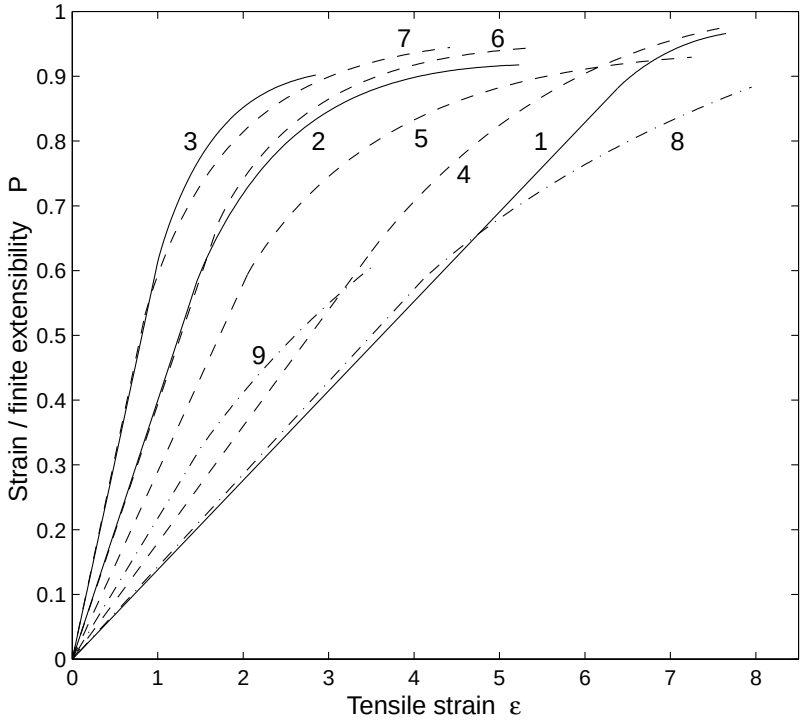

Fig. 10. Dependence of P on strain. (1) GF Kraus; (2) MT50 Fed; (3) Hf60 Amb; (4) VHS60 Pol; (5) V40 S05; (6) V40 S2; (7) SBR B SG; (8) SBR B; (9) SBR D.

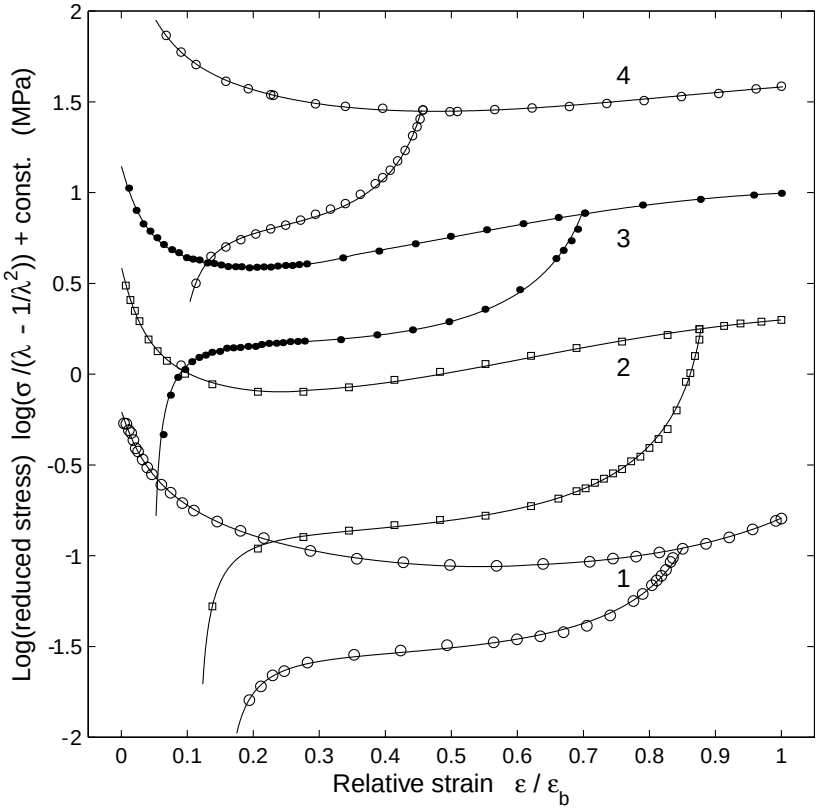

Fig. 11. Comparison of experimental virgin SSDs up to break and of experimental SSDs measured on retraction from strain ε_{max} (points) with the JGmC2L equation (curves), for one unfilled and three filler-reinforced networks. Coordinates log(reduced stress) and relative strain normalized with respect to strain-at-break. (1) SBR 0: (2) V40 S05; (3) Hf60 Amb; (4) SBR B SG. Vertical shift of data and curves, 3: + 0.3, 4: + 1.0.

of 20 MPa or higher. On the other hand, relaxational mechanisms are virtually absent in the unfilled network SBR D; its P_b is only 0.6 and the stress-at-break very low, 2.2 MPa.

3.5. Elongation–retraction cycle of networks containing various types of fillers

Fig. 11 shows the virgin dependences of log(reduced stress) on strain normalized with respect to strain-at-break, for one unfilled, very lightly crosslinked network and for three networks reinforced with precipitated silica, HAF carbon black and in situ generated silica, respectively. The graph also shows the retraction curves obtained with other specimens of the respective networks that were pre-extended only to a strain ε_{max} lower than strain-at-break. Data characterizing the experimental conditions of retraction and the tensile set TS at the end of retraction are given in Table 5 together with the parameters of the JGmC2L equation for the retraction curves. The individual elastomeric materials differ widely in their properties but, after normalizing with respect to the strain at break, all four extension–retraction dependences appear to be qualitatively very similar. The differences between them are a matter of degree rather than kind, in spite of the fact that apparently different relaxational mechanisms operate in individual networks: highly retarded elastic response in the unfilled, very lightly crosslinked network and a combination of polymer viscoelasticity with slipping processes at the polymer/silica, polymer/carbon black, and polymer/in situ silica interface, respectively, in the filled networks, with particle–particle forces intervening at low strains. The result shown in Fig. 11 suggests that a theoretical calculation of the stress-strain dependences of real elastomeric materials probably does not need to rely on molecular models of too specific a character.

Table 5
Parameters of the JGmC2L equation for retraction and other characteristics of variously reinforced networks

Parameter	SBR A	V 40 S05	Hf 60 Amb	SBRB SG
n	0.30	1.0	1.40	1.0
C_1 (MPa)	0.0125	0.063	0.22	0.205
C_2 (MPa)	0.047	0.060	0.21	0.250
λ_m	11.7	6.66	2.97	2.78
ε_b	14.18	7.25	2.85	4.42
ε_{max}	11.91	6.35	2.0	2.02
$\varepsilon_{max}/\varepsilon_b$	0.84	0.876	0.70	0.45_7
TS	2.2	0.85	0.14_2	0.36_5
TS/ε_b	0.15_5	0.11_7	0.05	0.08_3

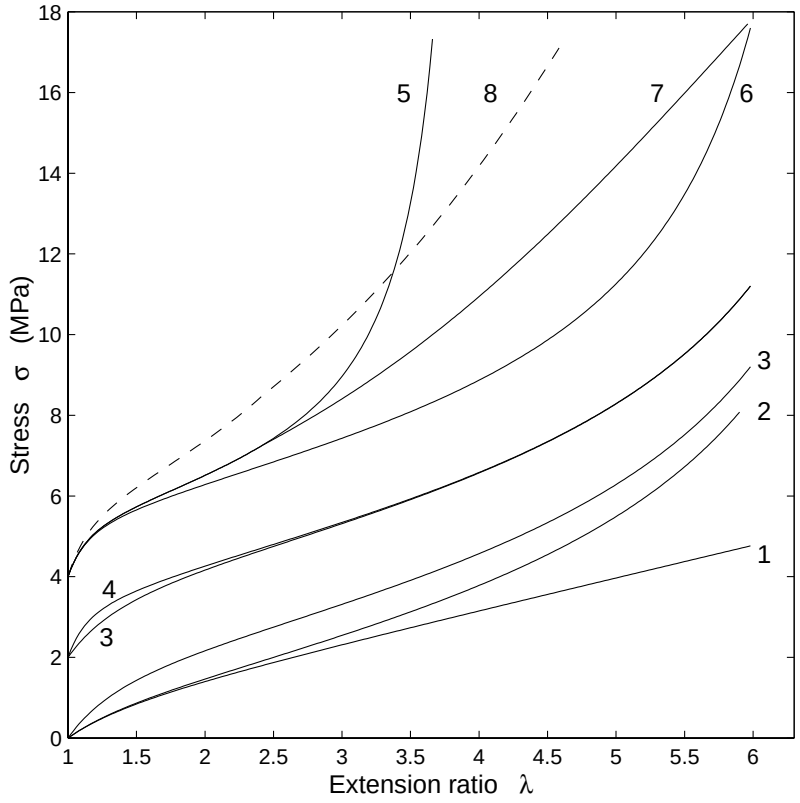

Fig. 12. SSDs calculated using the JGmC2L equation, Eqs. (A1) and (A2), to illustrate the effects of parameter values which are given in Table 6. Vertical shifts of the curves: 1–3: 0; 3,4: +2 MPa; 5–8: +4 MPa.

4. Conclusions

The JGmC2L combination of the James–Guth equation with the modified C_2 term of the Mooney–Rivlin equation and with the assumption of a strain-dependent finite extensibility parameter is able to describe, with a satisfactory accuracy, the virgin SSD up to the break of filler-reinforced SBR networks. The JGmC2L equation contains six adjustable and two additional parameters.

The parameter n is determined by the degree of curvature of the SSD at low strains. It increases with filler concentration and sensitively reflects changes in filler particle-particle interconnectivity, e.g. the effects of pre-strain, of graphitization of carbon black and of surface hydrophobization of silica.

The parameter C_1 which is predicted by theory to depend on the concentration of elastically effective network chains (stable network junctions), increases with increasing concentration of the filler reflecting at the same time its properties (e.g. particle size); it also reflects changes in the crosslinking degree of the matrix caused by the interaction of the filler surface with the crosslinking system.

Table 6
Parameter values for curves 1–8 drawn according to the JGmC2L equation, Eqs. (A1) and (A2), in Fig. 12 (Special cases of the JGmC2L equation: GT, Gaussian elasticity-theory equation, Mooney–Rivlin equation $C_2 \neq 0$, $n = 1$, λ_m infinite; JG, James–Guth equation; JGC2: JG equation + C_2 term; JGmC2, JG equation + modified C_2 term; JGmC2L: JGmC2 equation with a λ-dependent finite extensibility parameter. Note: the finite extensibility parameter for curves 2–6 is independent of λ, i.e. $\lambda_{m,2} = \lambda_m$)

Parameter	1	2	3	4	5	6	7	8
n	–	–	1	3	3	3	3	3
C_1	0.4	0.4	0.4	0.4	0.4	0.4	0.4	0.6
C_2	0	0	0.4	0.4	0.4	0.4	0.4	0.4
λ_1	–	–	–	–	–	–	2.4	2.4
$\lambda_{m,1}$	–	–	–	–	–	–	4	4
λ_2	6	6	6	6	3.7	6	6	4.7
$\lambda_{m,2}$	infinite	8	8	8	4	7	7	5.7
a	–	–	–	–	–	–	1.2	1.2
Equation	GT	JG	JGC2	JGmC2	JGmC2	JGmC2	JGmC2L	JGmC2L

The parameter C_2 of conventionally reinforced networks is distinctly less dependent than C_1 on factors like the filler type and concentration, crosslinking degree of the matrix, and effect of pre-strain. Therefore, a very high C_2/C_1 value (~25) has been obtained in a lightly crosslinked network with 30 phr of silica while with increasing filler concentration and crosslinking degree, C_2/C_1 tends to diminish to less than unity. Silica generated in situ by the sol–gel process imparted an unusually high C_2, much larger than those obtained in conventional filler reinforcement. This can be interpreted on the basis of the slip-link theory by assuming that contributions to C_2 stem from all possible slipping processes including sliding of polymer–polymer contacts (entanglements), polymer–filler contacts and also filler–filler contacts which in our sol–gel network apparently were formed in large amounts.

The $\lambda_{m,1}$ parameter indicates the beginning of the finite extensibility upturn effect. Inherent in the present treatment is the assumption of a strain-induced increase of λ_m (i.e. of network mesh size) to a larger value, $\lambda_{m,2}$, reached at break. As can be expected, both $\lambda_{m,1}$ and $\lambda_{m,2}$ decrease with increasing filler concentration and increasing crosslinking degree of the matrix. The relative change, D, of $(\lambda_m - 1)$ on extension up to break tends to increase with the filler concentration decreasing with graphitization of carbon black and hydrophobization of silica surface. A satisfactory correlation of $\lambda_{m,2}$ with C_1 was found for most networks and its comparison with theoretical predictions leads to a reasonable estimate of molar mass of the statistical segment.

When compared in the coordinates of log(reduced stress) vs. strain normalized with respect to strain-at-break, the extension–retraction curves of one unfilled and three filled networks containing silica, HAF black and in situ silica, respectively, show the same general features of the stress-strain behaviour, the differences being a matter of degree rather than kind.

Acknowledgements

The authors are greatly indebted to the Grant Agency of the Czech Republic for financial support of this work within the Grant Project No. 203/98/0884.

Appendix A

Definitions and equations:

σ is the nominal tensile stress (force per unit of undeformed cross-sectional area).

λ is the extension ratio; ratio of extended and unextended length L/L_0; $\varepsilon = \lambda - 1$ is the tensile strain; $\sigma_{red} = \sigma/(\lambda - 1/\lambda^2)$ is the reduced stress.

Mooney–Rivlin equation:

$$\sigma = 2C_1(\lambda - 1/\lambda^2) + 2C_2(1 - 1/\lambda^3)$$

where C_1 and C_2 are elastic constants (adjustable parameters).

Modified C_2 term, mC2:

$$2C_2(1 - 1/\lambda^{3n})$$

n adjustable parameter reflecting the degree of curvature of the SSD at strains ca. 0–100%.

JGmC2 equation:

$$\sigma = 2C_1(\lambda_m/3)\{\mathscr{L}^{-1}(\lambda/\lambda_m) - (1/\lambda^{3/2})\mathscr{L}^{-1}(1/\lambda^{1/2}\lambda_m)\} + 2C_2(1 - 1/\lambda^{3n}) \quad \text{(A1)}$$

where λ_m is the finite (or limiting) extensibility parameter, i.e. the hypothetical highest possible extension ratio; $\mathscr{L}^{-1}$ is the inverse Langevin function; $\mathscr{L}(x) = \coth(x) - 1/x$ the Langevin function.

JGmC2L equation:

JGmC2 equation where the λ_m parameter is λ-dependent.

Dependence of λ_m on λ is obtained from the comparison of the JGmC2 equation with experimental data; it can be described by the following power function with parameters λ_1, λ_2, $\lambda_{m,1}$, $\lambda_{m,2}$ and a

$$\lambda \le \lambda_1: \quad \lambda_m = \lambda_{m,1}$$

$$\lambda > \lambda_1: \quad \lambda_m = \lambda_{m,1} + (\lambda_{m,2} - \lambda_{m,1})\{(\lambda - \lambda_1)/(\lambda_2 - \lambda_1)\}^a \quad \text{(A2)}$$

For illustration, several SSD calculated from the JGmC2L equation, Eqs. (A1) and (A2), using the parameter values given in Table 6 are shown in Fig. 12.

References

[1] Meissner B. Polymer 2000;41:7827.
[2] Meissner B, Matějka L. Polymer 2000;41:7749.
[3] James HM, Guth E. J Chem Phys 1943;11:455.
[4] James HM, Guth E. Ind Engng Chem 1941;33:624.
[5] James HM, Guth E. J Chem Phys 1953;21:1039.
[6] Mooney M. J Appl Phys 1940;11:582.
[7] Rivlin RS. Philos Trans R Soc 1948;A241:379.
[8] Klüppel M, Heinrich G. Macromolecules 1994;27:3596.
[9] Kraus G. Angew Makromol Chem 1977;60/61:215.
[10] Fedors RF. In: Saltman WM, editor. The stereo rubbers. New York: Wiley, 1977 (chap. 12).
[11] Ambacher H, Strauss M, Kilian HG, Wolff S. Kautsch Gummi Kunstst 1991;44:1111.
[12] Bueche F. J Appl Polym Sci 1961;5:271.
[13] Ikeda Y, Tanaka A, Kohjiya S. J Mater Chem 1997;7:1497.
[14] Polmanteer K, Lentz CW. Rubber Chem Technol 1975;48:795.
[15] Ball RC, Doi M, Edwards SF, Warner M. Polymer 1981;22:1010.
[16] Erman B, Mark JE. Structure and properties of rubberlike networks. New York: Oxford University Press, 1997.
[17] Boyce MC, Parks DM, Argon AS. Mech Mater 1988;7:15.
[18] Wu PD, van der Giessen E. Mech Phys Solids 1993;41:427.